CONF-8809192--2

UCRL- 100616
PREPRINT

Pion Production in Relativistic Collisions of Nuclear Drops

UCRL--100616

DE89 009954

C. T. Alonso
J. R. Wilson
T. L. McAbee
J. A. Zingman

This paper was prepared for submittal
to American Institute of Physics
Third International Colloquium
on Drops and Bubbles
Monterey, California
September 19-21, 1988

September, 1988

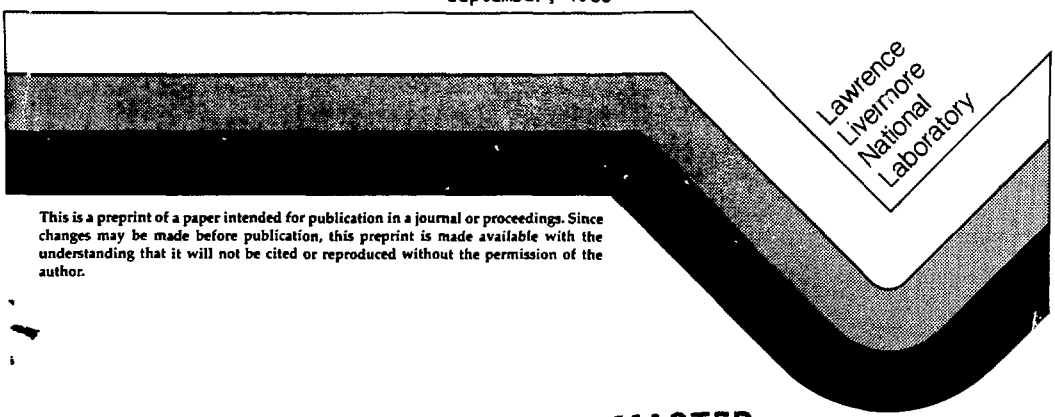

Pion Production in Relativistic Collisions of Nuclear Drops

C.T. Alonso, J.R. Wilson, T.L. McAbee, and J.A. Zingman
Lawrence Livermore National Laboratory,
Livermore, California 94550

In a continuation of the long-standing effort of the nuclear physics community to model atomic nuclei as droplets of a specialized nuclear fluid, we have developed a hydrodynamic model for simulating the collisions of heavy nuclei at relativistic speeds. Our model couples ideal relativistic hydrodynamics with a new Monte Carlo treatment of dynamic pion production and tracking. The collective flow for low-energy (200 MeV/N) collisions predicted by this model compares favorably with results from earlier hydrodynamic calculations which used quite different numerical techniques. Our pion predictions at these lower energies appear to differ, however, from the experimental data on pion multiplicities. In the case of ultra-relativistic (200 GeV/N) collisions, our hydrodynamic model has produced baryonic matter distributions which are in reasonable agreement with recent experimental data. These results may shed some light on the sensitivity of relativistic collision data to the nuclear equation of state.

---

1. Introduction

Ever since the discovery of nuclear fission, scientists have attempted, with remarkable success, to model the dynamics of atomic nuclei by assuming they behave like tiny drops of a nuclear fluid. In this fluid the strong nuclear force is analogous to the Van der Waals force of an ordinary liquid. Two main assumptions are made when a hydrodynamic model is applied to nuclear dynamics: (1) there are enough particles for the implied statistical nature of hydrodynamics to be valid (two fused uranium nuclei, for example, comprise 480 nucleons); and (2) the interaction distances are short compared to nuclear dimensions. This latter assumption is not well understood at present. Generally the nuclear force interaction length is approximately 1-2 fm (a fm or "fermi" is the unit of nuclear distance, equal to 10^{-13} cm) while the diameter of a heavy element nucleus is about 15 fm.

Since there is as yet no complete quantum description of relativistic heavy-ion collisions, we use macroscopic phenomenology to model the events that occur in these reactions. Many models have been proposed and investigated over the past decade, ranging from single particle models which attempt to mock up quantum effects, such as

quantum molecular dynamics[1] and VUU theories,[2] to collective models such as the hydrodynamics reported here.[3,4,13]

Relativistic nuclear collisions can be studied at several new and proposed facilities. Low energy (2 GeV/N, or lower, in the laboratory frame) collision data have been available since 1975 at the Bevalac accelerator in Berkeley. Mid-energy beams (15 GeV/N, lab) have recently become available at Brookhaven's AGS. Also during the last year data from the SPS at CERN have been available at 200 GeV/N (lab) or 60 GeV/N (lab). Proposed for the future is RHIC, a U.S.-based accelerator capable of 100 GeV/N in the center-of-mass frame. The push toward higher energies reflects the desire to create and explore the quark gluon plasma predicted at energy densities of several GeV/fm^3.[5]

2. Three-Dimensional Relativistic Hydrodynamics

The relativistic ideal-fluid hydrodynamics problem may be cast as a set of coupled nonlinear conservation equations: a continuity equation for baryon number density, an energy equation, and a momentum equation. The specific forms which we use are[6]

$$\partial_t(D) + \frac{1}{G}\partial_i\left(DGV^i\right) = 0, \tag{1}$$

$$\partial_t(E) + \frac{1}{G}\partial_i\left(EGV^i\right) + P\,\partial_t(\gamma) + \frac{P}{G}\partial_i\left(GU^i\right) = 0, \tag{2}$$

$$\partial_t(S_j) + \frac{1}{G}\partial_i\left(GS_jV^i\right) + \partial_j P = 0. \tag{3}$$

Here, γ is the Lorentz factor, $D = \rho\gamma$ is the coordinate density, $E = \rho\,\varepsilon\,\gamma$ is the internal energy density, $S_i = (D+E+P\gamma)\,U_i$ is the momentum density, ε is the specific internal energy and ρ is the density. P is the pressure, which is related to E and D through an equation of state. V^i is the transport velocity with respect to the coordinate grid, defined from the proper velocity U^i as $V^i = U^i/\gamma$. G is the square root of the determinant of the 3-metric. These forms differ slightly from those of other workers.[7] We solve these coupled, nonlinear equations using a monotonic continuous-fluid differencing scheme developed at Lawrence Livermore National Laboratory.[6,8,9] A second-order van Leer scheme is used for the advection terms. Momentum and baryon number are explicitly conserved. While energy is not explicitly conserved, it has been rigorously tested to accuracies of a few percent as described below.

Hydrodynamic modeling of a nuclear collision involves three physical processes. First, the lighter nucleus and the center of the heavier nucleus are stopped by a strong shock wave. Second, a weaker shock wave propagates outward from the shocked central region into the tangential surface region of the heavy nucleus. Third, the system expands adiabatically. To test whether our numerical algorithm is sufficiently accurate under similar conditions we calculated wall shocks, shock tubes, and rarefactions and compared the results to analytic solutions.[9,10,11]

To obtain accurate results at very high velocities (for example 200 GeV/N, with a relativistic factor $\gamma = 10$, corresponds to 0.995c in the equal speed frame) requires extremely careful treatment and testing of the solution scheme. We subjected our code to analytic shock tube tests, wall shock tests, and adiabatic expansion tests. Our typical accuracy was 1% to 3% in both the compression ratio and total energy conservation for a range of Lorentz factors from 1 to 10.

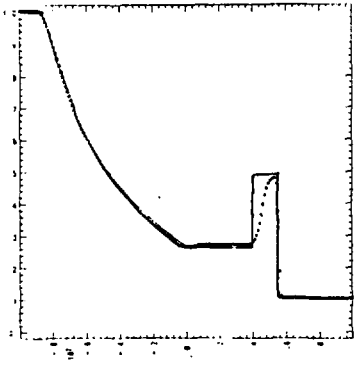

Figure 1. Shock tube test at 10 GeV/fm^3. Solid line: theory. Dotted line: code.

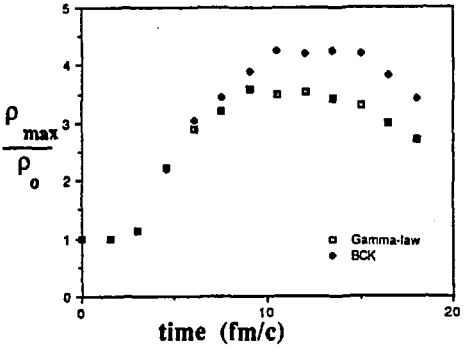

Figure 2. Maximum compression vs time for Au on Au at 200 MeV/N with two EOS's.

In Fig. 1 we present the results of the shock tube test at a specific energy of 10 GeV/fm^3 in the equal speed frame. For a rarefaction with this initial specific energy we obtain an error of less than 1% in the proper velocity down to an expansion ratio of 10 in density. The shock velocity is also found to better than 1% accuracy. In the absence of shock compression our code remains on an adiabat to one part in several thousand for compression ratios of order 10.

3. The Nuclear Equation of State

The equation of state (EOS) of nuclear matter has importance in both nuclear physics and astrophysics. In the latter, whether nuclear matter is soft or hard greatly affects the bounce of collapsing stellar cores, and can determine whether or not a supernova explosion occurs. In the former, whether nuclear matter is soft or hard is believed to greatly affect pion and quark-gluon plasma production in high energy collisions. As the internal energy in a nuclear system increases, it has been predicted that nuclear matter might undergo a phase transition resulting in a plasma consisting of bound quarks and the gluons which hold the nucleons together. The latent heat of vaporization from nucleons to quarks is estimated to be about 1-2 GeV/fm^3.[5]

At lower energies a quasi-empirical nuclear EOS parameterization has developed over the years. Most researchers use the so-called Skyrme[12] formula. We have used a very similar EOS which basically describes a relativistic baryonic Fermi gas with delta resonances included.[13] Our EOS was constrained to fit the known data, namely the nuclear binding energy and the compressibility and pressure of normal nuclear matter.

At higher energies we chose to use the gamma-law equation of state (EOS)

$$P = (\Gamma\text{-}1)\, E/\gamma, \qquad (4)$$

covering the range from moderately soft to very stiff EOS's. This choice seems appropriate because real sound speeds require $\Gamma > 1$ and causality limits require $\Gamma \leq 2$ at very high energies. One expects $\Gamma = 4/3$ for a quark gluon plasma at high energy, so a choice of $\Gamma = 4/3$ in particular seems well justified.

We used our code to study heavy ion collisions in both the low and high energy regimes.[13] At Bevalac energies (200 and 1350 MeV/N, $\gamma = 1.3$) nuclear compressions appear to be only marginally sensitive to changes in the nuclear matter EOS. In Fig. 2 we show the maximum compression as a function of time for Au on Au at 200 Mev/N using a hard and a soft EOS. The maximum compressions differ by about 15-20%. Given the large uncertainties in the experimental data it is hard to discriminate between such small differences.

At CERN energies (200 GeV/N, $\gamma = 10$), nuclear compressions during high-energy collisions appear to be more sensitive to changes in the nuclear EOS. While wall shock compression ratios are limited theoretically to the value of 4 for nonrelativistic $\Gamma = 5/3$ fluids, for relativistic fluids the maximum wall shock compression for $\gamma = 10$ and $\Gamma = 5/3$ is 27. Fig. 3 shows the maximum compressions calculated during the collision of ^{16}O and ^{208}Pb at 200 GeV/N as a function of time.

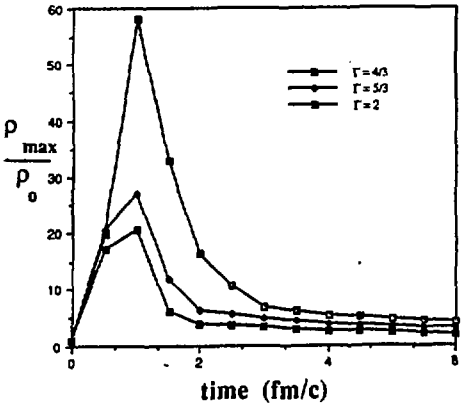

Figure 3. Maximum compression vs time for O on Pb at 200 GeV/N with Γ= 4/3, 5/3 and 2.

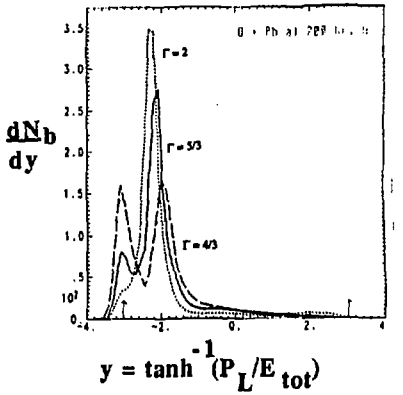

Figure 4. Differential baryon number vs rapidity for O on Pb at 200 GeV/N with Γ = 4/3. 5/3 and 2.

In Fig. 4 we show the quantity dN_b/dy vs. y for three different gamma-law EOS's ($\Gamma = 2$, 5/3, and 4/3). Here N_b is the number of baryons present and the "rapidity" y is defined by

$$y = \tanh^{-1}(P_L/E_{tot}), \qquad (5)$$

where p_L is the longitudinal momentum of a particle (fluid element) and E_{tot} is its total energy. Rapidity is a favored quantity for describing nuclear collisions because its transfer is an indication of the stopping power (as opposed to transparency) of colliding nuclear fluids. The three curves in Fig. 4 show a marked dependence upon the choice of nuclear EOS. There is a trend toward more baryons remaining at the initial rapidity for softer equations of state. For the $\Gamma = 4/3$ EOS we obtain baryon number densities greater than 20 ρ_O for a time of 0.8 fm/c. A maximum total energy density at peak compression of about 60 GeV/fm^3 is attained.

4. Pions as a Nuclear Fluid Signature

In the search for a sensitive indicator of the nuclear EOS, much interest has fallen upon the pions which are generated and propagated in hot dense nuclear matter. It is our hope that they will act as little thermometers. Pion generation in nuclear matter depends upon attaining a sufficiently high local energy density. The details are not very well known, but

the requirement is typically 0.2 GeV/fm^3. The scattering, absorption, and emission of pions depend upon the details of their interactions in hot dense nuclear matter and upon the equilibrium achieved. These details are not known in nuclear science today. We have been able to model these processes with the use of our pion code. This Monte Carlo pion overlay is now described below.

Pion production has heretofore only been investigated statically in chemical fluid models,[14,15] but our model treats the pions as dynamic Monte Carlo particles interacting with the baryonic fluid by exchanging momentum and energy during production, scattering, and absorption.[13] We define a master equation for the pion momentum distribution function,

$$\frac{dN_\pi(p_\pi)}{dt} = v_\pi \rho \sigma_A(\rho, p_\pi) f_{BE}(p_\pi, T) - v_\pi \rho \sigma_A(\rho, p_\pi) N_\pi(p_\pi)$$
$$- \rho N_\pi(p_\pi) \int v_{\pi N} \sigma_S(\rho, p_{\pi N}) D_B(p_N, T) d^3 p_N + \rho \int < v_\pi \sigma_S N'_\pi > d^3 p'_\pi \qquad (6)$$

Here N(p) is the distribution function, σ_A and σ_S the absorption and scattering cross-sections for pions from nucleons, respectively, and <> indicates a thermal average over the nucleon velocity in the fluid rest frame. Subscripts p denote pion quantities, while N indicates a nucleon. ρ is the baryon density, f_{BE} is the Bose-Einstein distribution, which we take to be the equilibrium solution for the model, and D_B is a relativistic Boltzmann distribution for the nucleons. Our model does not require equilibrium conditions; in fact, we have used the code to study approaches to equilibrium. The first term in the equation represents the production of pions by the thermal motion of the baryonic fluid. The second represents absorption of pions on pairs of nucleons. Note that these terms are taken so that detailed balance is guaranteed. The third term describes pion-nucleon scattering out of a given momentum state; the last term describes the scattering of pions with momentum p'_p into the state p_p by a thermalized baryon distribution.

In studying dynamic pions in this manner for the first time, we soon discovered that pions pose many interesting questions. For example, what are the details of pion generation in nuclear matter? Does scattering occur via the bare pion-nucleon cross section or the pions dressed? Will the pions scatter on each other? How soon is equilibrium reached? How transparent is the nuclear matter? What is the duration of the pion-baryonic matter interaction? At what energy do pions dominate the energy balance? Do other particles like kaons and delta resonances matter? How will phase changes in the nuclear matter affect pion production and transport?

While we have been able to explore answers to some of these questions with our code, many other questions remain unanswered. Some of our results are given below for the low energy and high energy regimes.

5. Low Energy (200 MeV/N and 1350 MeV/N) Simulations

Many experiments have been done at the Bevalac in the 200 MeV/N and 1350 Mev/N energy ranges. Analysis of the data shows that at these energies the colliding nuclear drops stop each other and impart considerable transverse momentum which results in "side splashing". We simulated such side splashing for Au on Au at 200 MeV/N with our code, as can be seen in Fig. 7b.

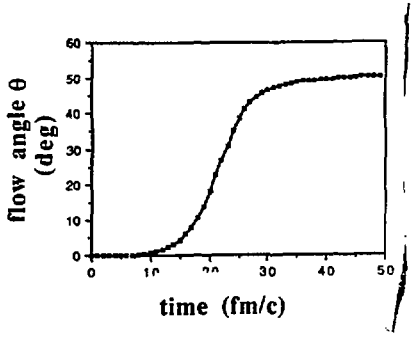

Figure 5. Flow angle vs time for Au on Au at 200 MeV/N.

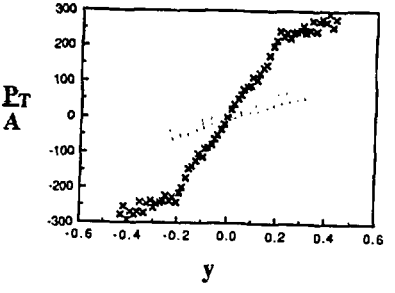

Figure 6. Transverse momentum vs rapidity for Au on Au at 200 MeV/N.

In Fig. 5 we show our prediction, as a function of time, for the flow angle for this collision. Since rapidity is a measure of stopping power, Fig. 6 shows the transverse momentum as a function of rapidity. The shaded line corresponds to deductions from experimental data. From experimental data the slope at zero rapidity has been deduced to be about 120 MeV/c.[16] Our hydrodynamic models, and those of other researchers, predict this slope to be more like 300 MeV/c. That is, in the low energy regime hydrodynamic models predict too much splash.

Figure 7a. Density plot for La on La at MeV/N at time 10 fm/c. The arrows show pion directions.

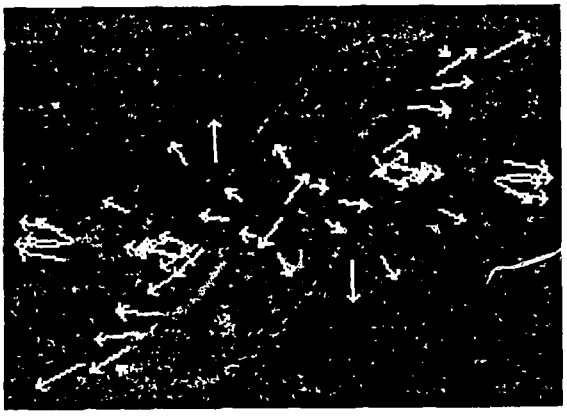

Figure 7b. Density plot for La on La at 13450 1350 MeV/N at time 15 fm/c. The arrows show pion directions.

We also calculated the dynamic pion production and tracking for La on La at 1350 MeV/N ($\gamma = 1.3$). We show in Fig. 7a and 7b our visual simulations, shaded in density, of the above reaction at times 10 fm/c (maximum compression) and 15 fm/c (separation).

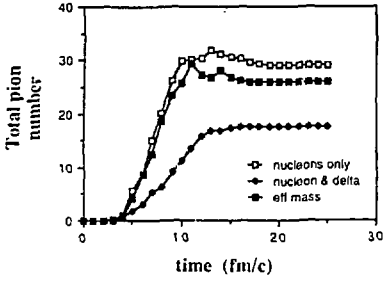

Figure 8. Pions vs time for La on La at 1350 MeV/N, for three different EOS's.

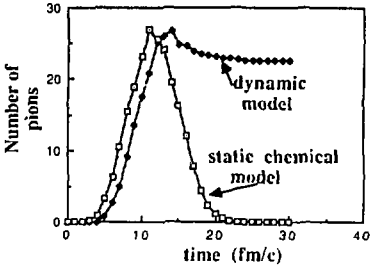

Figure 9. Pions vs time for La on La at 1350 MeV/N. Dynamic model compared to a static chemical model.

Fig. 8 shows the number of pions present in the calculation as a function of time for three different EOS's. Most of the pions are generated during the transit of the initial shock. The most pions we generated was around 30, whereas experimental deductions indicate about 50 in the actual collision. Thus our dynamic pion hydro model seems to underpredict the pion multiplicity by almost a factor of two while it overpredicts hydrodynamic splash by a factor of two.

We see a clue as to where the missing pions may come from in Fig. 9. We present here a time history of our pion production along with a static chemical model calculation in which the equilibrium number of pions was calculated in each cell and summed over the grid.[13] No pions from resonances were included. We observe that even though we do not force our system to assume an equilibrium solution, the number of pions at late times is very nearly that from the chemical model taken at maximum compression. We also observe a drop in the number of pions chemically produced at late times when the system expands and cools. The drop in the dynamic model comes from reabsorption of produced pions. We therefore conclude that we may be underpredicting with respect to the observed pion number [17] because we do not have a channel for pion production from resonance decay. Inclusion of a mean field such that the pion energy $E_\pi (\rho, p_\pi)$ is a function of the baryon density ρ as well as the pion momentum p_π is also an important improvement which is in progress.

6. High Energy (200 GeV/N) Simulations

Newly available heavy-ion beams at the CERN SPS[18,19] have sparked much interest in the behaviour of hot hadronic matter at high compression. Predictions of a transition to a new phase of baryonic matter, the quark-gluon plasma, require that energy densities reach several GeV/fm^3. It has also been suggested that nuclei may be partially to completely transparent to each other in very high energy collisions.[20,5] Early experimental results[18,19] for the collisions of ^{16}O with ^{208}Pb however, point to a high degree of stopping at lab energies of 200 GeV/N. This large stopping power may be indicative of hydrodynamic-like behavior in the collision systems.

Our calculations were performed in the equal speed system, so target and projectile rapidities were initially symmetric about zero. In this system, for the collision of ^{16}O (200 GeV/N in the lab) with ^{208}Pb, the Lorentz factor is 10.41. To obtain accurate results with

such high velocities (0.995c in the equal speed frame) requires extremely careful treatment and testing of the solution scheme.

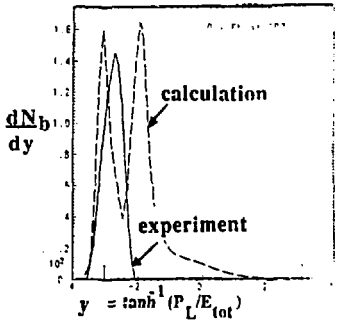

Figure 10. Differential baryon number vs rapidity for O on Pb at 200 GeV/N; our calculation compared to experiment.

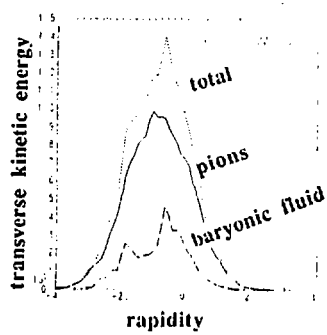

Figure 11. Transverse energy partition (GeV) between pions and baryons as a function of time for O on Pb at 200 GeV/N

In Fig. 10 we show the final-state baryon rapidity distribution for the collision of ^{16}O with ^{208}Pb at an energy of 200 GeV/N assuming a $\Gamma = 4/3$ EOS, for a calculation in which no pions were included. For the problem studied here y is initially 3.03 in the equal speed system. The numerical grid was 124 x 62 cells with dimension 0.067 x 0.167 fm^2 at the origin. Along the collision axis, geometric increases in cell size, with a ratio of 1.015, were employed to extend the grid. We ended our calculation at a time of 7 fm/c. The principal features of the rapidity distribution were not changing appreciably past 4.5 fm/c. Also shown in Fig. 10 is the experimental result[18] for ^{16}O collisions with a ^{197}Au target.

A striking feature of Fig. 10 is that about 60 nucleons remain at the initial Pb target rapidity. These nucleons represent a Pb corona (or "spectator fragment") which extends well beyond the original oxygen nucleus. The oxygen literally punches a hole in the lead, with formation of a weak radial shock. Thus, it is not surprising that an appreciable fraction of the Pb target remains at rest in the lab frame. Experimentally, about 65% of the total system mass is found to be localized (i.e. within one unit) about the initial target rapidity, compared with 70% for $\Gamma = 4/3$, 75% for $\Gamma = 5/3$, and 85% for $\Gamma = 2$ in our calculations. The remaining 35% of the experimental mass was not accounted for.[18]

We recently completed simulations that explicitly include the pion component. These preliminary runs, which have not been carried out far enough in time for pion generation to cease, indicate that about 300 pions are generated in ^{16}O with ^{208}Pb at 200 GeV/N. Since

an experimental number of 310 has been reported, we find this to be a remarkable preliminary agreement. We note that adding the pion component substantially changes the whole nature of the collision, as seen in the transverse energy plot shown in Fig. 11 and the rapidity curves in Fig. 12. Note the big difference in stopping power between Fig. 10 (pure hydro with no pions) and Fig. 12 (pions included). Our calculations indicate that the pions have captured fully 25% of the initial available energy. This is not surprising since the pion energies (1-2 GeV) are comparable to the baryon energies (10 GeV) in this frame. Indeed the pion number (300) at these high energy densities is greater than the nucleon number (224)!

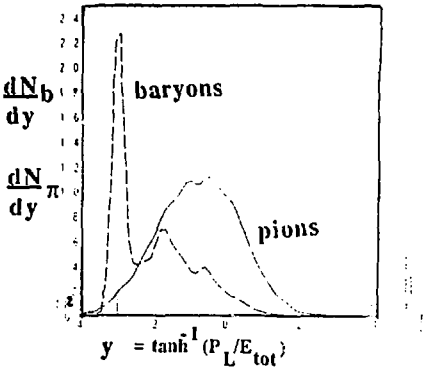

Figure 12. Differential baryon and pion numbers vs rapidity for O on Pb at 200 GeV/N. Solid line: pions.

Our runs have indicated that at these high energies pions are still generated at times well after shock transit has completed. This is in contrast to Bevalac runs where most of the pion generation occurs in the shocks. The reason is that at CERN energies the average energy density and compression remain high enough at late times for bulk pion production to continue (see Fig. 3). We have not yet been able to carry our calculations out long enough in time (past 10 fm/c) to see the end of the pion generation. In fact at their rather comparable speeds it may be almost impossible for the pion fluid to disengage from the nuclear fluid. At late times the CERN composite appears to be expanding at a Bevalac-like velocity.

The question arises whether the pions measured in the experimental detectors are providing information about the hot dense interior of the nuclear composite, where quark-gluon plasma may have formed, or whether the detectors only ob. ve pions that last interacted on the surface and carry little information about quark-gluon plasma. The answer

is not clear yet, but many of our pions appear to have had their last recorded interaction in regions of low density, presumably the surface regions. If so, then the pions may not be such useful little thermometers of the nuclear interior as we had hoped. It may be that kaons, which have a much smaller scattering cross section because they are strange, will prove to be more efficient carriers of the signature of the hot dense nuclear interior. We plan eventually to include kaons in our model.

Summary

We have made the following conclusions about hydro model simulations of low-energy (200 MeV/N) heavy ion collisions: (1) hydrodynamic flow predictions, using very different numerical approaches, are similar; (2) the hydrodynamic simulations overpredict the magnitude of the collective flow by about a factor of two in slope at zero rapidity; (3) including dynamic pion tracking with hydrodynamics underpredicts the pion multiplicity by almost a factor of two, 30 (theory) to 50 (experiment); and (4) including viscosity and a pion decay channel for delta resonances may correct these discrepancies.

Concerning high-energy (200 GeV/N) collisions, our hydrodynamic model appears to give qualitative agreement with the data. Hydrodynamic simulations reproduced the general features of the measured rapidity shift and pion multiplicity. These preliminary results indicate that the stopping power in such high energy collisions remains significantly high. We found that highly relativistic calculations require extremely careful treatment and testing. The relativistic composite appears to generate pions over long periods of time, long after the shock transit time. The energy balance is almost dominated by the pions, which have captured 25% of the available energy from the baryonic fluid.

While ideally the stopping power should be theoretically derivable directly from the nuclear force, in practice experience has shown that only experimental data can provide real insight into the behavior of such complex systems. Our hydrodynamic model provides a base for direct comparison with experimental data. Such physical processes as partial transparency and phase changes still need to be included. However, gross features such as baryon rapidity distributions and transverse kinetic energy have in fact been qualitatively described by our model. We conclude that our approach of overlaying Monte Carlo pion dynamics on a hydrodynamics base appears to have some utility.

This research was performed at Lawrence Livermore National Laboratory under the auspices of the United States Department of Energy, contract No. W-7405-Eng-48.

REFERENCES

1. J. Aichelin, H. Stöcker, Phys. Lett. 176B,14 (1986).
2. H. Kruse, B.V. Jacak, J.J. Molitoris, G.D. Westfall, H. Stöcker, Phys. Rev. C 31, 1770 (1985); H. Kruse, B.V. Jacak, H. Stöcker, Phys. Rev. Lett. 54, 289 (1985); J.J. Molitoris, H. Stöcker, Phys. Rev. C 32, 346 (1985).
3. A. A. Amsden, G.F. Bertsch, F.H. Harlow, J.R. Nix, Phys. Rev. Lett. 35, 905 (1975); G. Buchwald, G. Graebner, J. Theis, J. Maruhn, W. Greiner, H. Stöcker, Phys. Rev. Lett. 52, 1594 (1984).
4. J. Zingman, T. McAbee, J. Wilson, C. Alonso, LLNL Report UCRL-97153 (1987); J. Zingman, T. McAbee, J. Wilson, C. Alonso, LLNL Report UCID-21126 (1987).
5. L. McLerran, Rev. Mod. Phys. 58, 1021 (1986).
6. J.F. Hawley, L.L. Smarr and J.R. Wilson, Ap. J. 277, 296 (1984).
7. H. Stöcker and W. Greiner, Phys. Rep. 137, 277 (1986); R.B. Clare and D.Strottman, Phys. Rep. 144, 177 (1986).
8. J.R. Wilson and G.J. Mathews, in Conference Proceedings, "Frontiers in Numerical Relativity", Champagne, Illinois, 1988, to be published.
9. J. Centrella and J.R. Wilson, Ap. J. Supp. 54, 229 (1984).
10. K.W. Thompson, J. Fluid Mech. 171, 365 (1986).
11. J.F. Hawley, L.L. Smarr and J.R. Wilson, Ap. J. Supp. 55, 211 (1984).
12. H. Stöcker, W. Greiner, Phys. Rep. 137, 277 (1986).
13. J.A. Zingman, T.L. McAbee, J.R. Wilson and C.T. Alonso, Phys. Rev. C 38, 760, (1988).
14. H. Stöcker, W. Greiner, W. Scheid, Z. Phys. A286, 121 (1978); P. Danielewicz, Nucl. Phys. A314, 465 (1979).
15. D. Hahn, H. Stöcker, Nucl. Phys. A452, 723 (1986).
16. J.W. Harris *et al.*, LBL-23476 (1987).
17. J.W. Harris *et al.*, Phys. Rev. Lett. 58, 463 (1987).
18. H. Schmidt et al. (WA80 Collaboration), in "Proceedings of the 27th International Summer School for Theoretical Physics", Zakopane, Poland, 1986, to be published.
19. A. Bamberger et al. (NA35 Collaboration), Phys. Lett. B184, 271 (1987), R. Albrecht et al. (WA80 Collaboration), Phys. Lett. B199, 297 (1987).
20. J.D. Bjorken, Phys. Rev. D27, 140 (1983).